ARTICLE NO. 79-1477R

Study of Viscous Crossflow Effects on Circular Cylinders at High Reynolds Numbers

W. D. James*
Iowa State University, Ames, Iowa
S. W. Paris†
Boeing Aerospace Company, Seattle, Wash.
and
G. N. Malcolm‡
NASA Ames Research Center, Moffett Field, Calif.

Experimental studies on the viscous crossflow over circular cylinders for Reynolds numbers from 0.14×10^6 to 10.9×10^6 at Mach numbers of less than 0.3 were conducted in the 12-ft pressure wind tunnel at NASA Ames Research Center. Cylinder diameters were varied to determine the effect of the ratio of surface roughness to model diameter on the sectional drag coefficient. Data indicated that as the ratio of roughness to diameter decreased to around 3×10^{-6} cm/cm, the values of drag coefficient were asymptotically approaching some lower limit. Results also indicated that in the transcritical region the drag coefficients were slightly below previous values and were still rising for increasing Reynolds number at Reynolds numbers up to 11×10^6. Strouhal numbers were also below the previous values found at the larger Reynolds numbers. Partial results from the study of the dynamic variation of surface pressure coefficients indicated that at any specific angular position there was a decrease in surface pressure variation about the mean pressure for increasing body diameter and for increasing Reynolds number above 7×10^6. Data also indicated that nonuniform spanwise transition between flow regimes was the cause of the variability found in the behavior of the fluid flow around the cylinders.

Nomenclature

c_d	= crossflow static section drag coefficient
c_p	= section pressure coefficient
D	= cylinder diameter, cm
f	= wake shedding frequency, Hz
fD/V	= Strouhal number
k	= rms surface roughness, cm
M	= crossflow Mach number
Rn	= crossflow Reynolds number based on model diameter
Rn_δ	= crossflow Reynolds number based on surface roughness
V	= freestream velocity, cm/s
θ	= angular position referenced to forward stagnation point, deg

Introduction

THERE are two areas of fluid mechanics problems that are currently of high interest. One is the aerodynamic lift and drag on circular and noncircular bodies at high angles of attack such as missile bodies and aircraft fuselages. Another is the crossflow drag characteristics of two-dimensional bodies (primarily of circular cross section) in water such as the cold water pipe which is part of the proposed Ocean Thermal Energy Conversion System (OTEC). For both cases, the success in describing the flow details and resulting forces are, to varying degrees, dependent upon measurements of the viscous crossflow at high Reynolds numbers over circular cylinders. Because of limitations in the availability of test facilities capable of obtaining low Mach number, high Reynolds number results, the quantity of such data is limited,[1-7] with only one known source[3] providing results at Reynolds numbers based on a diameter above 8.6×10^6. The present paper presents results from an experimental program conducted in the 12-ft pressure wind tunnel at NASA Ames Research Center to provide sectional drag coefficient data at the higher Reynolds numbers. The tests were conducted over a range of Reynolds numbers from 0.15×10^6 to 10.9×10^6 at Mach numbers of less than 0.3.

The objectives of the research program were fourfold. The first was to obtain low Mach number crossflow drag coefficients at Reynolds numbers up to at least 10^7, and to observe the changes in drag coefficient due to the variation in the ratio of surface roughness to model diameter k/D. The second objective was to study the behavior of the boundary layers and to measure the variation of the Strouhal number with variation in Reynolds number. As with the crossflow drag coefficients, measurements such as these have only been made once before at Reynolds numbers above 10^7. The third objective arose when studies concerning the type and size of endplates that should be used disclosed that apparently no tests had been conducted on the effects of endplates on the flow around bluff bodies. It was, therefore, decided to include such tests in the program. The fourth and final objective was to study the effect of tunnel blockage on drag measurements on bluff bodies and to compare the blockage corrections proposed by Maskell[8] with those currently being used in the 12-ft pressurized tunnel. Results to be presented will be limited to those from the first and second objectives above. Results from the third and fourth objectives are included in Ref. 16.

Presented as Paper 79-1477 at the AIAA 12th Fluid and Plasma Dynamics Conference, Williamsburg, Va., July 23-25, 1979; submitted Aug. 14, 1979; revision received Feb. 20, 1980.

Index categories: Subsonic Flow; Nonsteady Aerodynamics; Boundary-Layer Stability and Transition.

*Associate Professor, Dept. of Aerospace Engineering. Member AIAA.

†Engineer, Engineering Flight Technology Staff. Member AIAA.

‡Research Scientist, Aerodynamics Research Branch. Member AIAA.

Experimental Arrangement

Test Facility

The wind tunnel tests were conducted in the 12-ft pressure wind tunnel at NASA Ames Research Center. For this facility the maximum unit Reynolds number occurs at a Mach number of approximately 0.29, and for that reason tests were conducted at that value. The maximum unit Reynolds number that could be obtained with the present models was approximately 24.6×10^6/m (7.5×10^6/ft).

Models and Instrumentation

To accomplish the above objectives, three circular cylinders with diameters of 15.24, 31.65, and 45.16 cm (6.0, 12.46, and 17.78 in.) were machined from extra heavy, seamless "black" pipe. The ratios of surface roughness to model diameter for the cylinders were 5.00×10^{-6}, 1.85×10^{-6}, and 3.09×10^{-6} cm/cm, respectively. The models spanned the test section horizontally and were mounted on flanges extending 43 cm into the tunnel. The flanges were covered, as shown in Fig. 1, with a cylindrical housing having a diameter equal to that of the model, and extending from the model to the tunnel wall when the 31.65- and 45.16-cm-diam models were tested. The cracks between the housing and model were covered with tape to prevent air leakage and in effect create two-dimensional models completely spanning the test section. However, since the diameter of the flanges to which the models were mounted was greater than the diameter of the 15.24-cm-diam cylinder, the flanges could not be covered to yield a two-dimensional model spanning the test section in the case of the smallest cylinder. Because of this, the 15.24-cm-diam cylinder was tested using circular endplates to isolate the model from any effect of the 6.0-cm-thick combined mounting flanges. Tests were run with two sets of 1.27 cm thick circular endplates with sharp edges to study the effect, if any, of varying the ratio of endplate diameter to cylinder diameter. The diameters of the circular endplates tested were 45.72 and 60.96 cm (18.0 and 24.0 in.), yielding endplate diameter to cylinder diameter ratios of 3 and 4, respectively.

The instrumentation on each model consisted of 18 static pressure ports evenly spaced at 20 deg increments about the circumference of the models near their centerline, as shown in Fig. 2 (Sec. C). By rotating the models at 2 deg increments through a total rotation of 40 deg, pressure information were obtained at least twice per point at 2 deg increments around the cylinders. By integrating these pressure measurements, values of static sectional drag coefficient were obtained. This integration was done on line yielding two separate values of c_d for each 40 deg total rotation, one from the first 20 deg of rotation and the second from the final 20 deg. Also shown in Fig. 2 are the eight bands of static pressure ports (Sec. A) located at equally spaced stations between the model centerline and the end of the model. Each band consisted of five static pressure ports located at 30 deg intervals. These pressure ports served two purposes. When the 15.24 cm diam circular cylinder was tested, this instrumentation permitted a study of the spanwise variation of the flow as the ratio of endplate diameter to model diameter was varied. However, for the 31.65- and 45.16-cm-diam cylinders, with which no endplates were used, the pressure measurements provided an indication of the two-dimensionality of the flow over the center portion of the models.

In order to investigate unsteady phenomena on the surface of the cylinders, 12 Kulite pressure transducers were evenly spaced around the circumference near the model centerline (see Fig. 2, Sec. D). Output from these transducers was recorded on a 32-channel recorder for later study. Two hot wires were mounted approximately 1.6 m downstream of the centerline of the cylinders to yield shedding frequency data. The outputs of these hot wires were also recorded for later study. Surface shear measurements using surface-mounted hot wires were also made when testing the 31.65-cm-diam cylinder. Seven hot wires were placed at 30-deg intervals as shown in Fig. 2 (Sec. B). The results of these measurements are reported in Ref. 9.

The model surface was carefully cleaned prior to the initial run each day, with the process repeated each time the pressure chamber surrounding the test section was opened. Prior to final shutdown each day, the model was coated with CRC 3-36 "Surface Protection for Metals" to prevent surface contamination from rust or corrosion.

Test Results

Variation of Static Surface Pressure Coefficient with Angular Position and Reynolds Number

The general nature of flow around a circular cylinder, as well as the variation in drag coefficient caused by this flow,

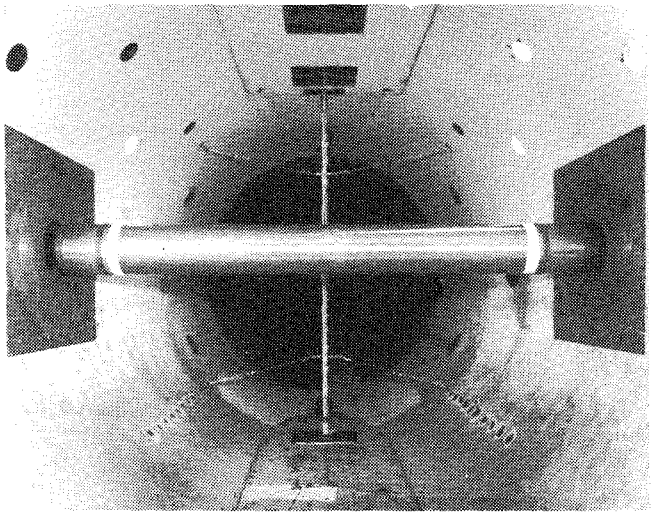

Fig. 1 Photograph of the 31.65-cm circular cylinder in the NASA Ames 12-ft pressure wind tunnel looking downstream.

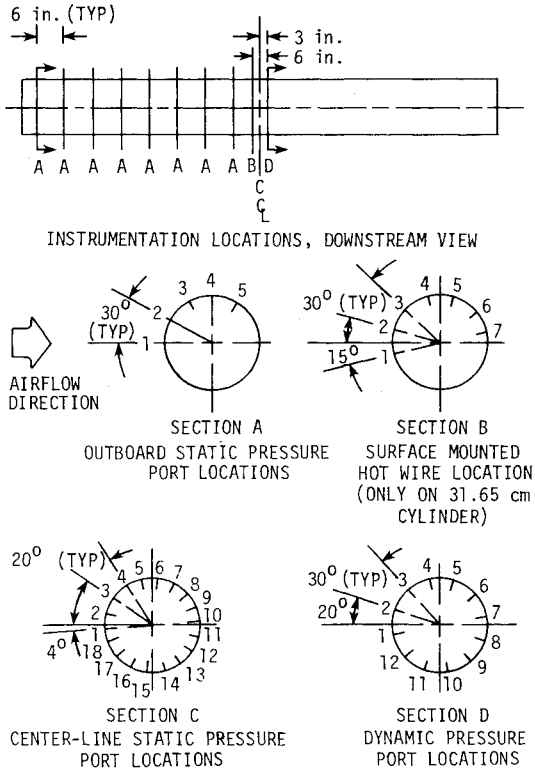

Fig. 2 Location of instrumentation on the 31.65-cm circular cylinder.

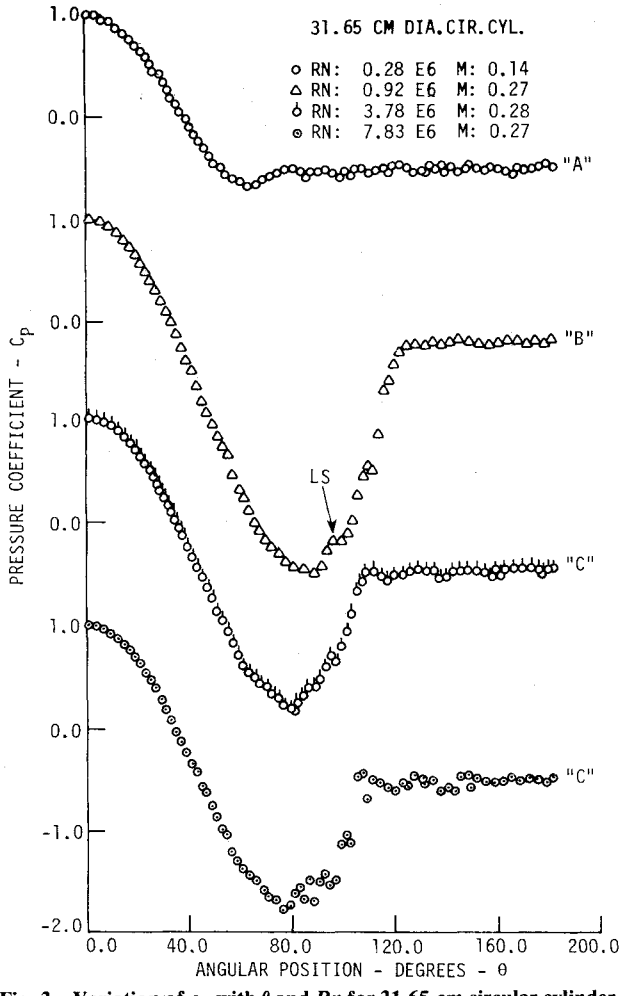

Fig. 3 Variation of c_p with θ and Rn for 31.65-cm circular cylinder.

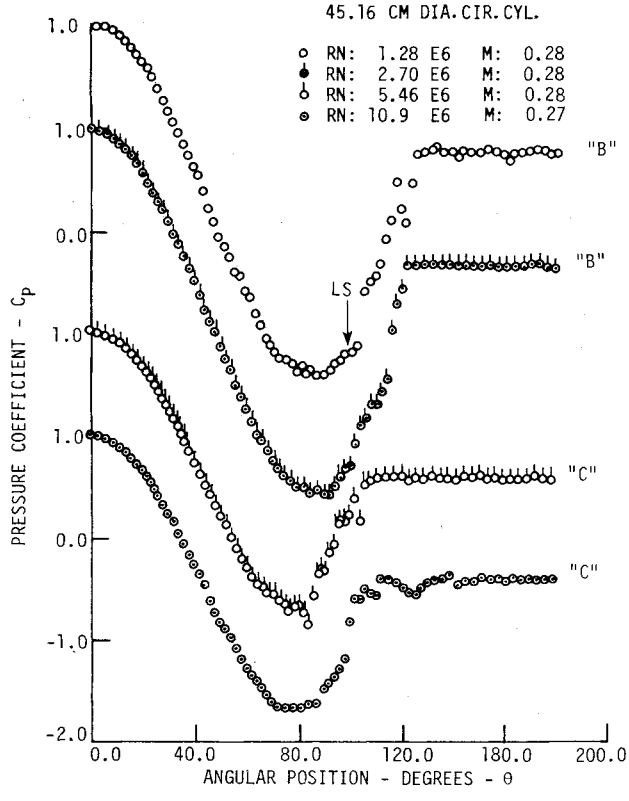

Fig. 4 Variation of c_p with θ and Rn for 45.16-cm circular cylinder.

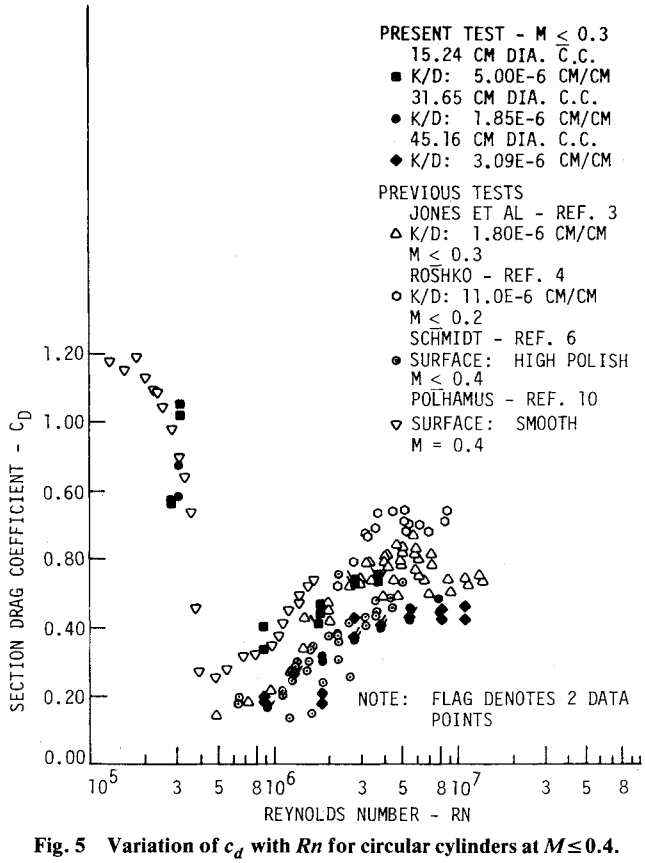

Fig. 5 Variation of c_d with Rn for circular cylinders at $M \leq 0.4$.

can best be pointed out by considering the changes in surface static pressure coefficient c_p, as both angular position θ around the cylinder and Reynolds number are varied. Figures 3 and 4 show this variation for Reynolds numbers from 0.28×10^6 to 10.9×10^6 from results obtained from the 31.65- and 45.16-cm-diam circular cylinders, respectively. From the plots in these figures, three distinct curve shapes are apparent: shape "A" with separation in the neighborhood of 80 deg aft of the forward stagnation point; shape "B" with separation occurring between approximately 120 and 130 deg aft of the forward stagnation point; and shape "C" with separation occurring between approximately 100 and 110 deg aft of the forward stagnation point. The nature of the flow accompanying each shape was first described by Roshko,[4] in which he broke the flow into four regimes which he called subcritical, critical, supercritical, and transcritical. This description will be used in this paper and can be summarized as follows.

The subcritical flow regime is located at Reynolds numbers below $1\text{-}2 \times 10^5$, where it is seen from Fig. 5 that the drag coefficient is leveling off at a value of approximately 1.2. It has long been agreed that in this Reynolds number range the flow over a circular cylinder is laminar, with a laminar separation occurring around 80 deg. The surface static pressure coefficient distribution accompanying this behavior is that of curve A. In the Reynolds number range from $1\text{-}2 \times 10^5$ to $4\text{-}5 \times 10^5$ the drag coefficient is rapidly decreasing from its previously constant value of 1.2 to a minimum value of from 0.16 to 0.3 depending upon the ratio of surface roughness to model diameter. Within this range the surface pressure coefficient variation changes from curve A to curve B as the point of minimum surface pressure coefficient moves rearward to approximately 85 deg and the separation point shifts rearward to beyond 120 deg (see Fig. 3). This is the critical regime.

Between Reynolds numbers of $4\text{-}5 \times 10^5$ and $2.5\text{-}4.0 \times 10^6$ is the supercritical regime. The shape of the c_p curve is that of

the B curve just discussed; however, as seen in Fig. 5, the drag coefficient begins to increase with increasing Reynolds number. In the first part of this range of Reynolds numbers it is presently believed[2-4] that there exists a laminar separation followed by transition, reattachment, and, finally, turbulent separation aft of 120 deg. This sequence appears on the surface static pressure coefficient curve as a small flat region on the backside prior to the final turbulent separation as indicated by LS in Figs. 3 and 4. Work by Achenbach[2] indicates that as the Reynolds number continues to increase, transition moves forward of the point of laminar separation and the bubble disappears. The Reynolds number at which this occurs is highly dependent on k/D. As indicated by the test results in Ref. 2, by the time a Reynolds number of 2.5-4.0$\times 10^6$ is reached, the transition point has moved well forward on the front side of the cylinder. As the transition point moves forward, the minimum value of c_p found on the cylinder becomes more positive, but the final separation still occurs aft of 120 deg.

Above Reynolds numbers of 2.5-4.0$\times 10^6$ the transcritical regime is reached and the third distinct curve, shape C, occurs. In this regime the point of minimum surface pressure coefficient moves forward from around 85 deg to around 78 deg, while the separation point moves forward from aft of 120 deg to between 100 and 110 deg, as can be seen by comparing the curves in Figs. 3 and 4. The section drag coefficient continues a slow increase but at a rate well below that of the supercritical regime. At present it is felt that this behavior will continue, with perhaps the drag coefficient reaching some upper limit as the Reynolds number continues to increase.

It must be noted that the boundaries between the above regimes, particularly the subcritical and critical and the supercritical and transcritical, are highly sensitive to both k/D and surface disturbances. This gives rise to two items that should be mentioned. The first is the fact that because of this sensitivity, flow around a cylinder is seldom symmetrical near the boundaries of the regimes called out above. For this reason it is dangerous to attempt to base drag coefficients on measurements taken over only one-half of the body surface. The second item arises from this "possibly symmetrical, possibly not" behavior and is the uncertainty in drag coefficient value near the supercritical-transcritical boundary. More will be said about this later.

Variation of Drag Coefficient with Reynolds Number and Surface Roughness

Figure 5 shows the variation of crossflow drag coefficient with Reynolds number for the three circular cylinders tested. Also shown on the plot are drag coefficients from the previous high Reynolds number tests of Jones et al.,[3] Roshko,[4] and Schmidt.[6] As with the previous data, the results appear to scatter over a wide band. However, when the ratio of surface roughness to model diameter k/D is considered, the results become much more consistent in their pattern. The 15.24-cm-diam cylinder with the largest ratio of surface roughness to model diameter $k/D=5.00\times 10^{-6}$ cm/cm, has the largest values of c_d. The 45.16-cm-diam cylinder with the next largest ratio of roughness to diameter, $k/D=3.09\times 10^{-6}$ cm/cm, tends to have values of c_d that lie in the middle, while the 31.65-cm-diam cylinder which has the smallest ratio of roughness to diameter, $k/D=1.85\times 10^{-6}$ cm/cm, has the smallest values of drag coefficient. However, the difference between the values of c_d for the last two cylinders probably lies within the range of uncertainty of the blockage corrections. This close proximity tends to indicate that as the ratio of roughness to diameter decreases to the neighborhood of 3×10^{-6} cm/cm and smaller, the values of c_d are asymptotically approaching some lower limit.

At a Reynolds number of approximately 1.8×10^6, this proximity of results fails to hold, with the 45.16-cm cylinder having a significantly lower c_d than the 31.65-cm cylinder. An explanation for this reversal of behavior can be found by considering the relative locations of the separation points on the two cylinders involved. It should be noted that the data being considered lie in the range of Reynolds numbers within which the variation of c_d has exhibited an increasing scatter in previous work. This is the range of Reynolds numbers just prior to the Reynolds number at which the separation point moves from approximately 125 deg forward to around 105 deg. This forward movement of the separation point causes an increase in drag coefficient due to the wider wake and, therefore, larger form drag. Achenbach[2] has shown that the Reynolds number at which this transition occurs is sensitive to surface conditions, suggesting that in the present tests the surface conditions on the 31.65-cm cylinder were such that the separation point was moving forward before a Reynolds number of 1.8×10^6 was reached, while for the 45.16-cm cylinder, separation was still at the rear position. This suspicion is confirmed by the data plotted in Fig. 6, where the angular position of the separation point, obtained from static pressure distribution data, is plotted vs Reynolds number for the 31.65-cm and 45.16-cm cylinders. The separation locations on both the upper and lower surfaces of the cylinders are shown. The resulting graph indicates that the angular locations of the separation point fall within a band, the center of which starts around 75 deg in the subcritical regime, increases to the neighborhood of 125 deg in the low supercritical regime, and then falls to around 105 deg as the Reynolds number is increased into the transcritical regime. At a Reynolds number of 1.8×10^6, the figure shows that the wake of the 31.65-cm cylinder is wider than that of the 45.16-cm cylinder, thereby yielding a larger drag coefficient.

It also should be noted that the drag coefficients of the 31.65-cm cylinder did not exhibit a peak in the neighborhood of a Reynolds number of 5×10^6 as did the drag coefficients from the cylinder of Jones et al.[3] having the same value of k/D. Unlike the data of Jones et al., which show a decreasing drag coefficient for increases in Reynolds numbers beyond 5×10^6, data from the present tests indicate that the drag coefficient is still rising slightly for increasing Reynolds number at Reynolds numbers up to 11×10^6.

Szechenyi[11] has suggested a technique to remove the scatter present in c_d with models having different surface roughness to model diameter ratios in which he plots c_d vs a roughness Reynolds number Rn_δ, where the characteristic length in the Reynolds number is the size of the roughness, in his case the

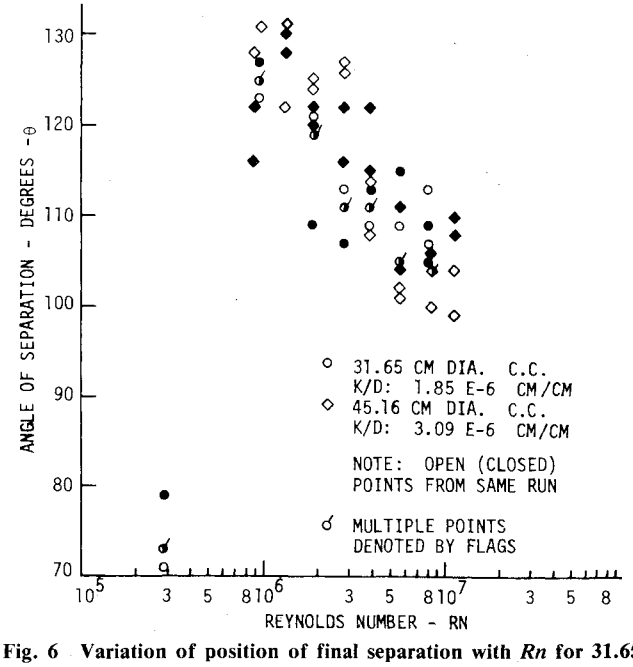

Fig. 6 Variation of position of final separation with *Rn* for 31.65 and 45.16-cm circular cylinders.

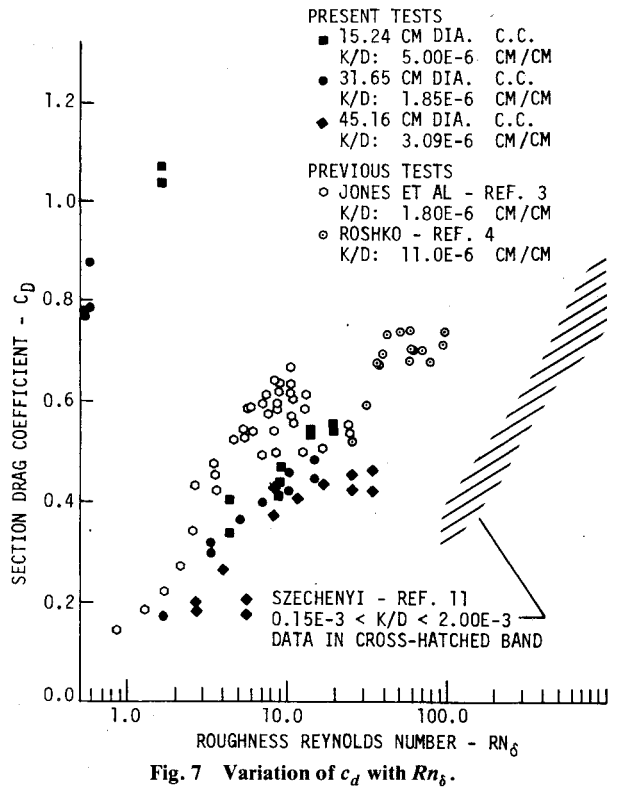

Fig. 7 Variation of c_d with Rn_δ.

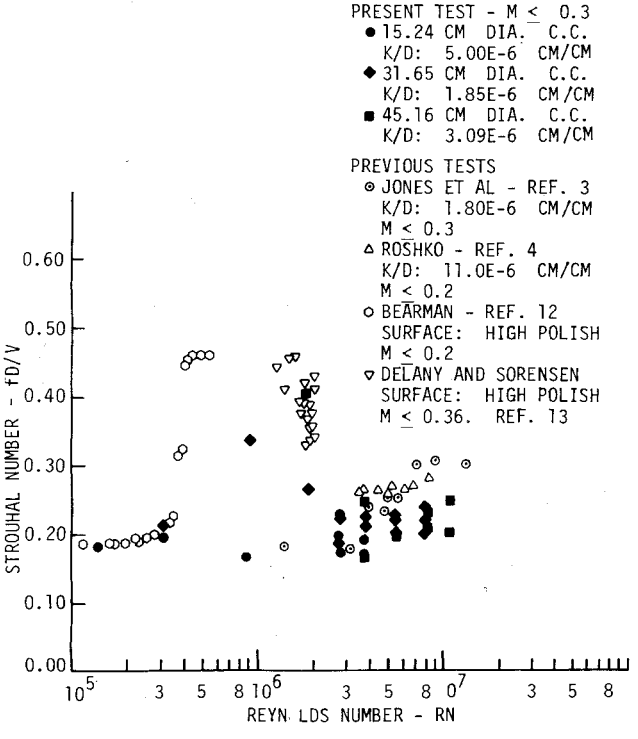

Fig. 8 Variation of Strouhal number with Rn.

diameter of the beads he used for roughing the surface. Figure 7 shows such a graph where c_d is plotted against the roughness Reynolds number. As pointed out by Szechenyi, the results lie in a band along a common line. However, Fig. 7 points out the need for a better method of defining roughness size, since for machine-finished surfaces, as in the case for the present models, the roughness must be measured in terms of rms cm taken in the direction of the spanwise axis of the model instead of diameters of applied beads or coarseness of a layer of sand. Probably due to the lack of common measure of

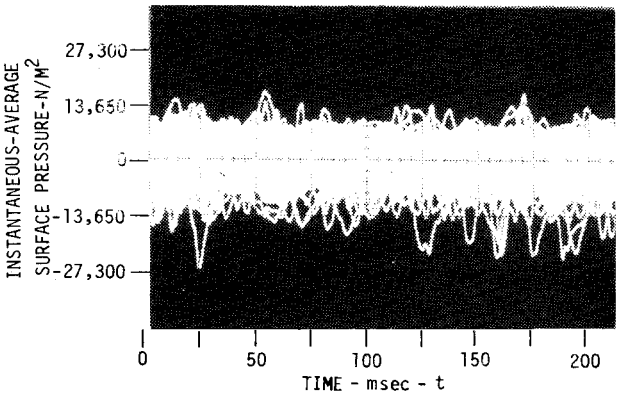

Fig. 9 Fifteen-second time exposure of dynamic variation of surface pressure.

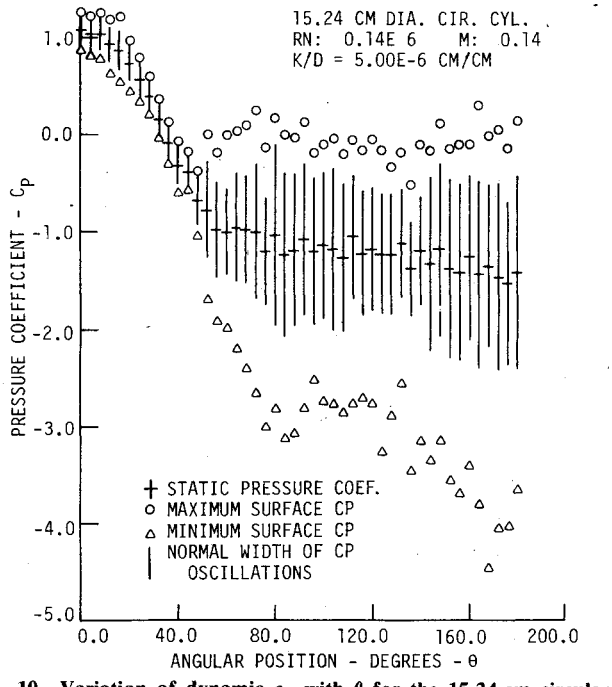

Fig. 10 Variation of dynamic c_p with θ for the 15.24-cm circular cylinder at $Rn = 140{,}000$.

roughness, the results of this investigation and those of Jones et al.[3] and Roshko[4] are shifted significantly to the left of the corresponding results presented by Szechenyi.

Variation of Strouhal Number with Reynolds Number

Figure 8 shows the variation of Strouhal number with Reynolds number. Shedding frequencies were measured by two hot wires mounted 1.60 m downstream of the model centerline. This yielded a distance from the rear surface of the models to the hot wires of 10, 4.56, and 3.04 diameters for the 15.24-, 31.65-, and 45.16-cm-diam models, respectively. Also shown in the figure are the results of Jones et al.,[3] Roshko,[4] Bearman,[12] and Delany and Sorensen.[13] Jones obtained his Strouhal numbers using a frequency determined from the frequency of the autocorrelation function of the time-history data samples of his unsteady lift force. Roshko, Bearman, and Delany and Sorensen obtained their shedding frequency as was done in this report, by using instrumentation mounted downstream of the rear of their cylinders a distance of 6.8, 1, and 1-1.5 diam, respectively. Again, the results of this investigation agree well with those of past investigations, except at the higher Reynolds numbers where the present results fail to show as great an increase as in previous investigations.

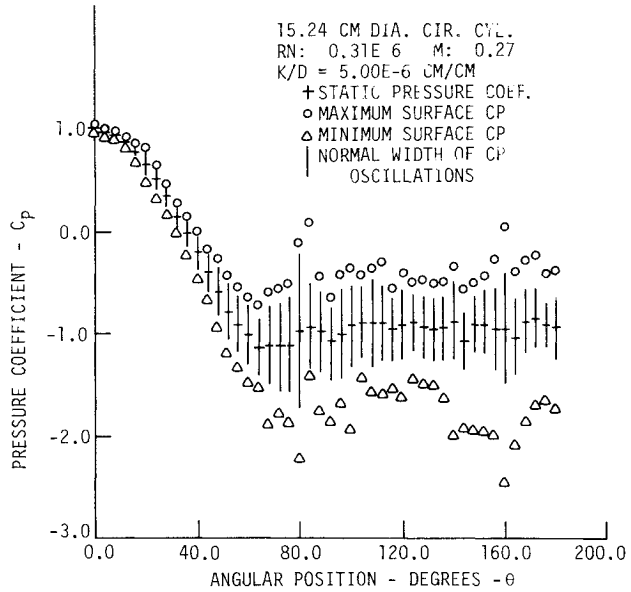

Fig. 11 Variation of dynamic c_p with θ for the 15.24-cm circular cylinder at $Rn = 310{,}000$.

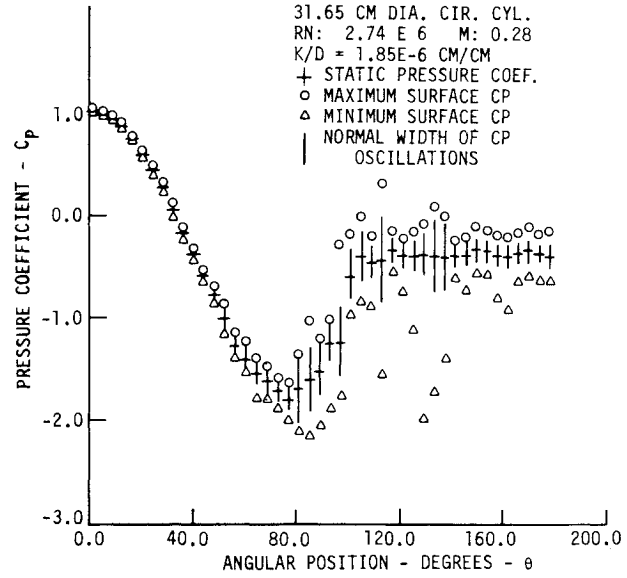

Fig. 14 Variation of dynamic c_p with θ for the 31.65-cm circular cylinder at $Rn = 2{,}740{,}000$.

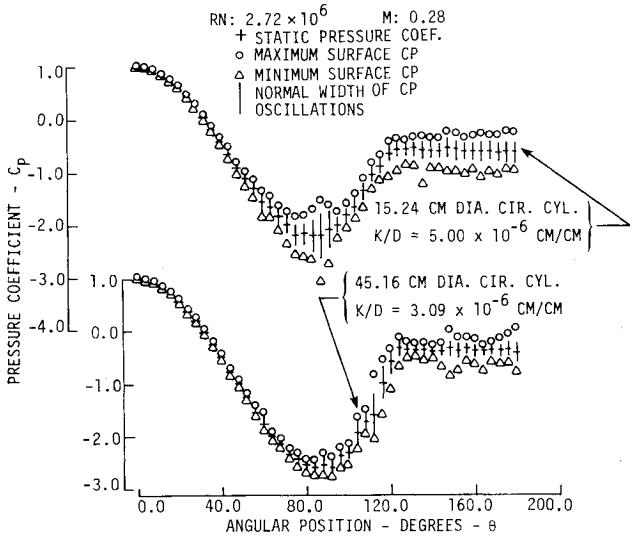

Fig. 12 Variation of dynamic c_p with θ for the 15.24- and 45.16-cm circular cylinder at $Rn = 2{,}720{,}000$.

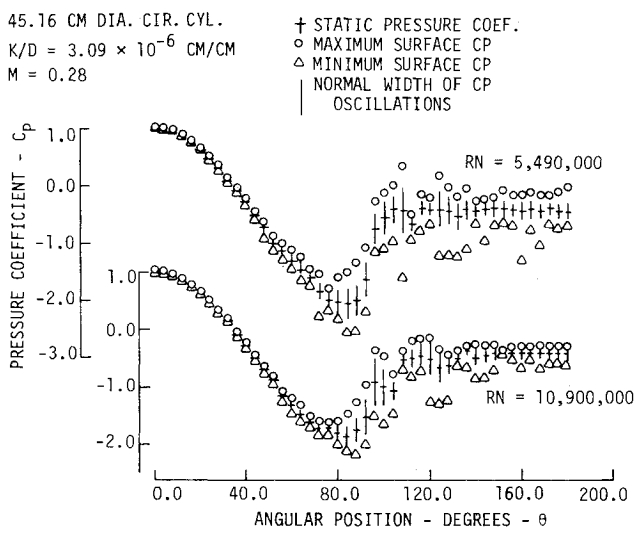

Fig. 13 Variation of dynamic c_p with θ for the 45.16-cm circular cylinder at $Rn = 5{,}450{,}000$ and $10{,}900{,}000$.

There are two points in Fig. 8 that need to be discussed. A Strouhal number of 0.34 was found for the 31.65-cm cylinder and a Strouhal number of 0.17 was found for the 15.24-cm cylinder in the Reynolds number range around 0.9×10^6. Both lie in the supercritical regime where the Strouhal vs Reynolds number curve exhibits a flat-topped hump having a maximum Strouhal number of approximately 0.45, and just to the left of the accepted transition to the transcritical regime at which the Strouhal number rapidly decreases to between 0.2 and 0.3. The Strouhal numbers were based on frequencies obtained from hot-wire signals that exhibited a single, distinct spike that did not correspond to a tunnel or hot-wire mount natural frequency. At present, the authors are at a loss to explain their presence other than to suggest it might be connected to the early transition from the supercritical to transcritical regimes, as will be discussed in the next section. It should be noted that Jones et al. have also reported a Strouhal number of 0.182 at a Reynolds number of 1.38×10^6, which is also in the supercritical regime.

Dynamic Variation of Surface Pressure

The study of the dynamic pressure variation and the boundary-layer behavior has not yet been completed. However, Figs. 10-12 show the variation in pressure coefficient from the mean value over one-half of the cylinder circumference for Reynolds numbers from 0.14×10^6 to 2.72×10^6, subcritical to critical regimes, for the 15.24-cm cylinder, while Figs. 12 and 13 show the variation for Reynolds numbers from 2.70×10^6 to 10.9×10^6, supercritical to transcritical regimes, for the 45.16-cm cylinder. In obtaining the variations shown in these figures, a study was made of a 15-s segment of the recorded output for each of the Kulite pressure transducers at every angular position for which data were recorded. For a given model and angular position, the corresponding segment was displayed on an oscilloscope and a time exposure photograph was made of the complete 15-s segment (see Fig. 9). From this time exposure, three values were measured: the solid bandwidth or width of the band that appeared solid due to repeated coverage by the transducer output during the 15 s; the maximum value on the exposure or the peak value of the signals that appeared above the solid band; and the minimum value on the exposure or the negative peak value of all the signals that appeared below the solid band. The "maximum surface c_p" and the "minimum surface c_p" values plotted were the pressure coefficients calculated using the maximum and minimum values,

respectively. The "normal width of c_p oscillations" plotted is the range of pressure coefficients between the pressure coefficients calculated using the values at the upper and lower limits of the solid band. These results were then plotted at the desired angular position assuming the known static surface pressure coefficient would lie at the center of the "normal width of c_p oscillations." Only three other sources of such results are known[5,14,15]; however, only in Ref. 5 are data included for the supercritical regime. From Figs. 10-12 it can be seen that as the Reynolds number increases from the subcritical regime into the critical regime, the variation in pressure coefficient from the mean value undergoes dramatic changes. At a Reynolds number of 0.14×10^6 (Fig. 10), there is a large variation from 50 deg rearward, while from 0 to 50 deg, the variation decreases. When the Reynolds number is increased into the critical regime to 0.31×10^6 (Fig. 11) and then on to 2.72×10^6 (Fig. 12), the overall variation on the surface of the cylinder decreases.

This same trend is exhibited by the 45.16-cm cylinder in the supercritical regime as shown in Fig. 12. Figure 13 shows the behavior in the transcritical regime. Here it is seen that from approximately 45 deg rearward there is an increase in the variation of pressure coefficient with increases in Reynolds number. The variation reaches a maximum at a Reynolds number around 5.5×10^6, after which the variation decreases with increasing Reynolds number. Throughout both the supercritical and transcritical regimes there is no significant variation between $\theta=0$ and 45 deg.

Figures 12 and 14 show the variations in pressure coefficient for the three cylinders, $D=15.24$, 45.16, and 31.65 cm, respectively, tested at a Reynolds number of approximately 2.73×10^6. These figures show that in general the variation in static pressure coefficient decreases with increasing diameter. However, as in previous comparisons, there are narrow angular bands in which the above generality does not hold, such as between $\theta=130$ and 140 deg where the 31.65-cm cylinder has the largest variation.

Conclusions

The above test results at Reynolds numbers greater than 7×10^6 mark only the second time that crossflow drag data have been obtained at Reynolds numbers this large for circular cylinders with surface roughness to cylinder diameter ratios below 4×10^{-6} cm/cm. The drag coefficients are slightly below those of the previous work, while the Strouhal numbers fail to show the large rise previously found at the larger Reynolds numbers. The c_d results followed the previously predicted pattern when plotted against a roughness Reynolds number, but the shift between present and past results clearly points out the necessity of establishing a standard technique for defining surface roughness, a technique that encompasses the machine finish of the real world as well as the sand and spherical body finishes found in the laboratory.

The first-known plots of variation of surface pressure coefficients with angular position at Reynolds number above 7×10^6 were also included.The results indicate that at any specific angular position there is a decrease in surface pressure variation about the mean pressure for increasing body diameter and for increasing Reynolds number above 7×10^6.

Perhaps the most important observation to be drawn from the present tests is the variability in the behavior of the fluid flow around a circular cylinder, especially in the supercritical regime. Although test results could not explain why this variability occurred, test data did show it was due to nonuniform spanwise transitioning between flow regimes. Results further indicated that this behavior diminishes as the test Reynolds number departs from the supercritical regime.

Acknowledgments

This work was supported by the Engineering Research Institute of Iowa State University through funds provided by NASA Ames Research Center under Grant NSG-2091.

References

[1] Achenbach, E., "Distribution of Local Pressure and Skin Friction Around a Circular Cylinder in Cross-Flow Up to $Re=5\times10^6$," *Journal of Fluid Mechanics*, Vol. 34, 1968, Pt. IV, pp. 625-639.

[2] Achenbach, E., "Influence of Surface Roughness on the Cross-Flow Around a Circular Cylinder," *Journal of Fluid Mechanics*, Vol. 46, 1971, Pt. II, pp. 321-335.

[3] Jones, G. W., Jr., Cincotta, J., and Walker, W., "Aerodynamic Forces on a Stationary and Oscillating Circular Cylinder at High Reynolds Numbers," NASA TR R-300, Feb. 1969.

[4] Roshko, A., "Experiments on the Flow Past a Circular Cylinder at Very High Reynolds Number," *Journal of Fluid Mechanics*, Vol. 10, 1961, Pt. II, pp. 345-356.

[5] Van Nunen, J.W.G., "Pressure and Forces on a Circular Cylinder in a Cross-Flow at High Reynolds Number," Proceedings, *Symposium on Flow-Induced Structural Vibrations*, Karlsruhe, Germany, 1972.

[6] Schmidt, L. V., "Fluctuating Force Measurements Upon a Circular Cylinder at Reynolds Numbers up to 5×10^6," NASA TMX-57,779, June 1966.

[7] Morkovin, M. V., "Flow Around Circular Cylinder—A Kaleidoscope of Challenging Fluid Phenomena," *Symposium on Fully Separated Flows*, edited by Arthur G. Hansen, American Society of Mechanical Engineers, May 1964, pp. 102-118.

[8] Maskell, E. C., "A Theory of the Blockage Effects on Bluff Bodies and Stalled Wings in a Closed Wind Tunnel," Reports and Memorandum No. 3400, 1965.

[9] Murthy, V. S. and Rose, W. C., "Surface Shear Stress Measurements on Circular Cylinders in Cross-Flow at Near Critical Reynolds Numbers," NASA TM-78, 454, Jan. 1978.

[10] Polhamus, E. C., "Effect of Flow Incidence and Reynolds Number on Low-Speed Aerodynamic Characteristics of Several Noncircular Cylinders with Applications to Directional Stability and Spinning," NACA Tech. Rept. R-29, Sept. 1957.

[11] Szechenyi, E., "Supercritical Reynolds Number Simulation for Two-Dimensional Flow Over Circular Cylinders," *Journal of Fluid Mechanics*, Vol. 70, 1975, Pt. III, pp. 529-540.

[12] Bearman, P. W., "On Vortex Shedding From a Circular Cylinder in the Critical Reynolds Number Region," *Journal of Fluid Mechanics*, Vol. 37, 1969, Pt. III, pp. 577-585.

[13] Delany, N. K. and Sorensen, N. E., "Low Speed Drag of Cylinders of Various Shapes," NACA Tech. Note 3038, Aug. 1953.

[14] Cantwell, B. J., "A Flying Hot Wire Study of the Turbulent Near Wake of a Circular Cylinder at a Reynolds Number of 140,000," Ph.D. Thesis, California Institute of Technology, Pasadena, Calif., 1976.

[15] Hove, D., Shih, W., Albarro, E., "Hydrodynamic Design Loads for the OTEC Cold Water Pipe," SAI-79-559-LA, Prepared for National Oceanic and Atmospheric Administration under Contract NDBO-03-78-G03-050, Sept. 1978.

[16] James, W. D., Paris, S. W., and Malcolm, G. N., "A Study of Viscous Cross-Flow Effects on Circular Cylinders at High Reynolds Numbers," AIAA Paper 79-1477, Williamsburg, Va., July 1979.